^{67}Zn Mössbauer investigation of lattice-dynamical effects and hyperfine interactions in ZnF_2

M. Steiner, W. Potzel, C. Schäfer, W. Adlassnig, M. Peter,
H. Karzel, and G. M. Kalvius
Physik-Department (E15), Technische Universität München, James-Franck-Strasse, D-8046 Garching bei München, Federal Republic of Germany
(Received 25 September 1989)

The temperature dependence of lattice-dynamical effects and of hyperfine interactions in $^{67}ZnF_2$ has been investigated between 4.2 and 55.3 K with use of the 93.3-keV Mössbauer resonance in ^{67}Zn. Within this temperature range the Lamb-Mössbauer factor decreases from 1.23% to 0.46%. The electric quadrupole tensor characterized by $eV_{zz}Q/h = +8.2\pm0.1$ MHz and $\eta = 0.15\pm0.02$ is independent of temperature. The data on the quadrupole tensor and on the Lamb-Mössbauer factor exclude a beginning ferroelectric transition, which was proposed to occur at low temperatures. The results on the isomer shift (relative to ZnO) and on the electric quadrupole tensor are in very good agreement with recent theoretical cluster calculations.

I. INTRODUCTION

Theoretical calculations, both of the band structure[1] as well as of the cluster type,[2,3] have contributed considerably to deepen our understanding of the electronic structure in zinc chalcogenides and in ZnF_2. Theoretical and experimental investigations of *s*-electron densities at the Zn site in ZnO, ZnS, ZnSe, and ZnTe and, in particular, of the electric field gradient in ZnF_2 demonstrated the importance of covalent contributions of 4*s*, 4*p* and 4*d* electrons to the chemical bond. This can most clearly be seen by the strong correlation between the *s*-electron density $\rho(0)$ at the Zn atom and the (Pauling) electronegativity of the ligand.[4,5]

In compounds with ligands of larger electronegativity the *s*-electron density $\rho(0)$ decreases since the direct contribution to $\rho(0)$ of the 4*s* electrons by far outweighs the shielding effect of 4*p* electrons.[6] This interpretation was further corroborated by high-pressure experiments on ZnS.[7] Also, ZnF_2 with the most electronegative ligand fits well into this picture. Furthermore, in ZnF_2 the electric-field-gradient (EFG) tensor is largely determined by the 4*p* and 4*d* electrons.[2,3,8] The point charge model,[9] which might be expected to hold for ionic compounds, can neither reproduce the sign of the EFG nor its asymmetry parameter.[8]

Not only from point of view of hyperfine interactions but also concerning lattice-dynamical effects, ZnF_2 displays interesting properties. This compound crystallizes with tetragonal rutile structure, where each Zn is surrounded by a distorted F octahedron.[10–12] Several physical properties show anisotropic behavior, e.g., the coefficients of thermal expansion at low temperatures,[13] the axial compressibilities, and the dielectric constants.[14] In addition, from the anomalous low-temperature behavior of elastic constants[15] it has been argued that a beginning ferroelectric transition should occur at ~4.2 K, which would be accompanied by a monoclinic distortion of the lattice.[15,16] Such a transition should manifest itself by a soft transverse optical mode in the phonon frequency distribution.

Both the appearance of a soft mode as well as anisotropic properties are expected to modify lattice-dynamical effects, in particular, the mean-square atomic displacement of Zn which can be determined by changes of the Lamb-Mössbauer factor (LMF). Lattice distortions would also alter the EFG tensor and *s*-electron density at the Zn site.

In the present paper we studied the temperature dependence of the Lamb-Mössbauer factor, the center shift, and the quadrupole interaction in ZnF_2 using the high-resolution 93.3-keV Mössbauer transition in ^{67}Zn. This resonance involves a γ transition between a spin-$\frac{1}{2}$ excited and spin-$\frac{5}{2}$ ground state. Since the excited state will not split under the interaction of an electric-field-gradient tensor, the quadrupolar hyperfine pattern is comparatively simple and easily interpreted. The spin of the ground state, on the other hand, is high enough to determine the complete EFG tensor. Isomer shifts *S* are prominent.[4,5,17] Furthermore, the resonance linewidth is extremely narrow due to the long half-life of the excited state. Thus EFG and *S* can be measured with a precision typical for microwave resonance methods.[18–20] The ^{67}Zn Mössbauer resonance has been demonstrated to be also highly sensitive to lattice-dynamical effects.[21,22] This is due to the relatively large transition energy and the light mass of the Mössbauer atom. Our results presented on ZnF_2 seem to confirm the expected anisotropy of the mean-square atomic displacements, but give no indications of a soft mode or a lattice distortion at low temperatures.

II. EXPERIMENTAL DETAILS

Measurements were carried out in transmission geometry using a piezoelectric quartz spectrometer. The basic design has been described earlier.[21] Some modifications were made to heat the ZnF_2 absorber. As

indicated in Fig. 1, the aluminum holder containing the $^{67}ZnF_2$ powder could be heated to elevated temperatures by a little heating coil. The assembly was surrounded by a Makrolon container which fitted to the piezoelectric drive unit[21] and provided good thermal insulation. The drive system containing source and Makrolon holder was suspended by soft springs inside a sealed stainless-steel container filled with He exchange gas at reduced pressure.[21] In this manner it was possible to keep the source temperature below ~ 18 K even at absorber temperatures of ~ 60 K. The temperatures of source and absorber were determined by semiconductor devices (see Fig. 1).

The $^{67}ZnF_2$ compound was prepared by reaction of ^{67}ZnO and a 30% excess of $NH_4 \cdot HF$ at 633 K in dry argon flow. It was verified by x-ray diffraction that the ZnF_2 powder absorber had the rutile-type tetragonal TiO_2 structure.[10–12] The absorber thickness was 757 mg $^{67}Zn/cm^2$; the absorber area was 0.916 cm^2.

As sources we used ^{67}Ga in ZnO single crystals. The ^{67}Ga (half-life of $T_{1/2}=78$ h) activity was produced *in situ* by 28-MeV proton bombardment of ZnO single crystals at the cyclotron of the Kernforschungszentrum Karlsruhe. The ZnO single crystals were squares of 6×6 mm^2 area and of 1 mm thickness. They were cut with the c axis perpendicular to the crystal faces. After irradiation the sources were annealed at ~ 970 K in oxygen atmosphere for ~ 6 h and thereafter slowly (~ 50 K/h) cooled to room temperature.

ZnO crystallizes in the hcp structure. Therefore an axially symmetric quadrupole interaction is present in the source. With the c axis being oriented parallel to the direction of observation of the γ rays, the emission spectrum consists of two lines separated by 4.789 μm/s,[18,23] the ratio of intensities being 2:1.[24,25] Unfortunately, we had to use this multiline source instead of the well-established single-line source ^{67}Ga in Cu. The reason is that the latter would produce a center shift (~ 200 μm/s) which is large compared to the quadrupole splitting (~ 50 μm/s) of ZnF_2. This would make the measurements ineffective since one would scan most of the time a velocity range which contains no information. In addition, the velocity calibration would become more difficult. For sources ^{67}Ga in ZnO maximal velocities of $\sim \pm 100$ μm/s are sufficient. The splitting of the emission line in ZnO is only a minor inconvenience which can easily be taken into account by the fitting procedure. Since the splitting parameters are precisely known, no additional uncertainties are introduced.

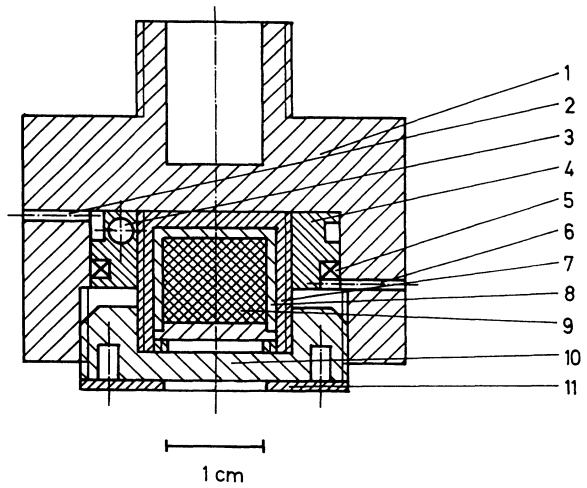

FIG. 1. Holder for heating the $^{67}ZnF_2$ absorber. 1, Makrolon holder; 2, hole for electrical leads (Si diode); 3, Si diode; 4, aluminum ring; 5, heating coil; 6, hole for electrical leads (heating coil); 7 and 8, absorber containers; 9, ZnF_2 powder absorber; 10, Makrolon cover; 11, Ta collimator.

The spectrometer was calibrated by replacing the $^{67}ZnF_2$ absorber by ^{67}ZnO powder leaving all other parts of the experimental setup unchanged. The resulting five-line pattern[24,25] was used for the velocity calibration.

To achieve Doppler velocities in excess of 100 μm/s for the ZnF_2 experiments driving frequencies of ~ 1000 Hz and sinusoidal driving voltages of $\sim 150 V_{\text{eff}}$ had to be employed. The calibration spectra were obtained at the same frequency. Although at such high frequencies transient effects[26,27] are clearly visible in the unfolded spectra, we found that after folding, the error of the velocity calibration induced by transient effects was only $\lesssim 0.4\%$. Together with the statistical accuracy, the five-line spectrum gave a precision of the velocity calibration of $\sim 1\%$. In contrast to the calibration measurements in the ZnF_2 experiments, Mössbauer absorption takes place at large negative velocities where the rate of change of velocity is already considerably smaller. Therefore transient effects are hardly visible even in the unfolded spectra and are unimportant after folding.

After being collimated by a tantalum disk of 1 mm thickness fastened to the Makrolon holder (see Fig. 1) the γ rays were detected by an intrinsic Ge diode of 10 mm thickness and 40 mm diameter coupled to a fast preamplifier. In order to achieve high counting speed and simultaneously good energy resolution, a fast double-differentiating main amplifier was used.[28] Count rates up to 160 000 s^{-1} in the 93.3-keV window were obtained. The signal-to-background ratio was typically $S/(S+B)\sim 65\%$. It was determined once a day by recording pulse-height spectra at the actual counting rate via a high-speed analog-to-digital converter.

III. RESULTS

A. Quadrupole interaction

Figure 2 shows the Mössbauer transmission spectrum measured at 4.2 K. The quadrupole splitting in ZnF_2 causes three widely separated hyperfine lines. As discussed in Sec. II, the splitting in the ZnO source results in two lines separated by ~ 4.8 μm/s with intensity ratio 2:1. Thus the observed spectrum consists of three pairs of lines, each pair reflecting the shape of the emission spectrum of the ZnO source. Figure 3 displays transmission spectra obtained at temperatures of ZnF_2 between 4.2 and 55.3 K. To display the details of the absorption lines only the velocity range between -30 and -105 μm/s is shown. The solid lines in Figs. 2 and 3 are least-squares fits of a superposition of three pairs of resonance lines. The Mössbauer parameters of the source

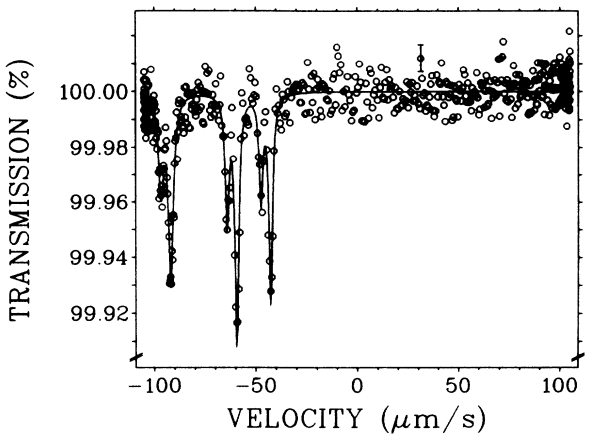

FIG. 2. Mössbauer spectrum of a $^{67}ZnF_2$ powder absorber measured with a ^{67}Ga in ZnO single crystal source, both at 4.2 K.

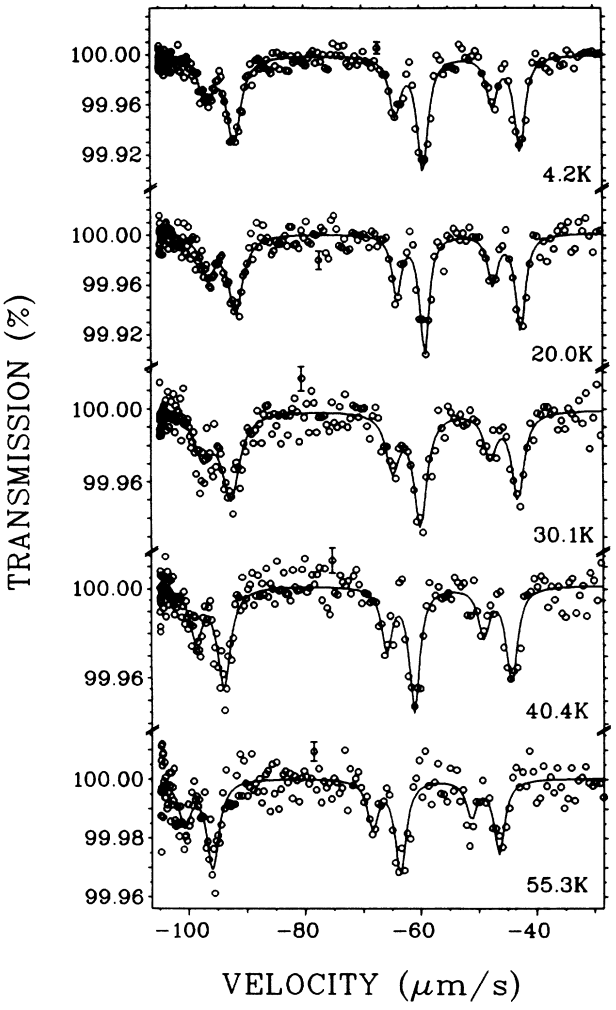

FIG. 3. Mössbauer absorption spectra obtained at temperatures of the $^{67}ZnF_2$ absorber between 4.2 and 55.3 K. The source is ^{67}Ga in ZnO single crystal kept at low temperature. Only the velocity range between -30 and -105 μm/s is shown. The full velocity range covers ± 105 μm/s as in Fig. 2.

emission spectrum (relative line intensities $=2:1$, line separation $=4.789$ μm/s) were kept fixed. In addition, within each pair the widths of both lines were assumed to be equal.

The results for the hyperfine splitting in the absorber are summarized in Table I. The linewidth [full width at half-maximum (FWHM)], the absorption area (depth $\times$ width), and the positions are given for the stronger absorption line of each of the three pairs.

The electric-field-gradient tensor is derived from the energy eigenstates of the $I=\frac{5}{2}$ level.[8,29] From the ratio of the energy separations $(E_{\pm 5/2}-E_{\pm 3/2})/(E_{\pm 3/2}-E_{\pm 1/2})$ the asymmetry parameter $\eta=(V_{xx}-V_{yy})/V_{zz}$ is calculated by solving the corresponding equation numerically. Using this value for η, the quadrupole frequency $\nu_Q=eV_{zz}Q/h$ can then be determined from the energy separation $E_{\pm 5/2}-E_{\pm 3/2}$ (or from $E_{\pm 3/2}-E_{\pm 1/2}$). With the known quadrupole moment of the spin-$\frac{5}{2}$ ground state $Q=+(0.150\pm 0.015)b$,[30] we can derive V_{zz}. Table II summarizes the results. As can be seen also from Fig. 4(a) the change of the quadrupole frequency with temperature up to 55.3 K is smaller than $\sim 1\%$. We get $\nu_Q=+(8.2\pm 0.1)$ MHz. As indicated by Fig. 4(b), the asymmetry parameter η appears to be constant with a possible slight increase at higher temperatures.

B. Center shift

A change with temperature of the center shift S_C is visible in Fig. 3. At absorber temperature $T_A=55.3$ K it has decreased by (3.86 ± 0.22) μm/s as compared to its value at 4.2 K after taking into account a small correction[25] due to the increase of the source temperature. As will be shown below, the center shift is mainly caused by the second-order Doppler shift.[31]

C. Lamb-Mössbauer factor

The Lamb-Mössbauer factor is derived from the total area under the absorption lines after correction for nonresonant background radiation. In addition, the temperature dependence of the recoil-free fraction $f_{\|}$ of the ZnO single crystal sources[25] was taken into account.

For an isotropic lattice and random orientation of the crystallites in the powder absorber, the relative areas under the three pairs of absorption lines are expected to be equal. For ZnF_2, however, this is not the case. As indicated by Fig. 5 the relative intensity of the innermost pair ($v\sim -40$ μm/s) is $\sim 20\%$ smaller than those of the other two pairs at all temperatures investigated. As will be discussed below this is mainly due to Goldanskii-Karyagin effect[32,33] originating from an anisotropic LMF. In addition, texture effects in the ZnF_2 powder are not negligible.

IV. DISCUSSION

A. Quadrupole interaction

Based on the anomalous temperature dependence of the elastic constants C_S and C_{44}, a ferroelectric transition

TABLE I. Summary of Mössbauer parameters for $^{67}ZnF_2$ at various temperatures T_A. The source is ^{67}Ga in ZnO single crystal kept at temperature T_S. Linewidth (FWHM), area (absorption depth × width), and position are given for the stronger absorption line of each of the three pairs. Only statistical errors are quoted. The center shift is given relative to its value at 4.2 K after applying a small correction for the temperature shift of the source.

T_A (K)	T_S (K)	Linewidth (μm/s)	Area (% μm/s)	Position (μm/s)	Center shift (μm/s)
4.2	4.2	2.91±0.15	0.202±0.007	−91.94±0.06	0
		2.22±0.13	0.209±0.008	−59.42±0.05	
		2.12±0.16	0.166±0.008	−42.65±0.06	
20.0	8.1	3.05±0.25	0.187±0.009	−91.71±0.10	+0.07±0.21
		1.88±0.16	0.182±0.010	−59.17±0.06	
		1.96±0.21	0.155±0.011	−42.58±0.08	
30.1	11.6	3.58±0.33	0.169±0.009	−92.67±0.13	−0.72±0.21
		2.74±0.29	0.169±0.011	−60.02±0.11	
		2.50±0.36	0.121±0.011	−43.17±0.14	
40.4	13.5	2.71±0.25	0.120±0.007	−93.93±0.10	−1.63±0.21
		2.14±0.24	0.119±0.009	−61.12±0.09	
		2.24±0.33	0.097±0.009	−44.31±0.13	
55.3	17.7	2.55±0.27	0.077±0.005	−95.97±0.11	−3.86±0.22
		2.25±0.35	0.072±0.007	−63.62±0.14	
		2.22±0.47	0.056±0.008	−46.59±0.18	

was proposed[15] to occur at low temperatures accompanied by a monoclinic distortion of the lattice. The extremely high energy resolution of the 93.3-keV resonance would be able to detect such distortions by changes of the hyperfine interactions. However, our data on the EFG tensor, the center shift, as well as on the Lamb-Mössbauer factor give no indications for a structural phase transition.

As demonstrated in Fig. 4 and Table II the electric field gradient is independent of temperature within ~1%, except for a possibly slight increase of η with temperature. The values for the EFG tensor at 4.2 K are in reasonable agreement with an earlier but less precise measurement.[18] Using $Q=+(0.150\pm0.015)b$ we derive $V_{zz}=+(2.25\pm0.23)\times10^{17}$ V/cm^2, $\eta=(0.15\pm0.02)$. The

TABLE II. Quadrupole interaction in $^{67}ZnF_2$ at various temperatures T_A. The quadrupole frequency $\nu_Q=eV_{zz}Q/h$ of the main component, the asymmetry parameter η, and the main component V_{zz} of the electric-field-gradient tensor are given. The errors quoted include a 1% uncertainty of the Doppler velocity. The error in V_{zz} arises mainly from the relatively large uncertainty of the quadrupole moment Q.

T_A (K)	ν_Q (MHz)	η	V_{zz} (10^{17} V/cm^2)
4.2	8.20±0.06	0.15±0.02	2.26±0.23
20.0	8.19±0.09	0.12±0.03	2.26±0.23
30.1	8.23±0.10	0.16±0.04	2.27±0.23
40.4	8.26±0.10	0.14±0.04	2.28±0.23
55.3	8.18±0.10	0.20±0.03	2.26±0.23

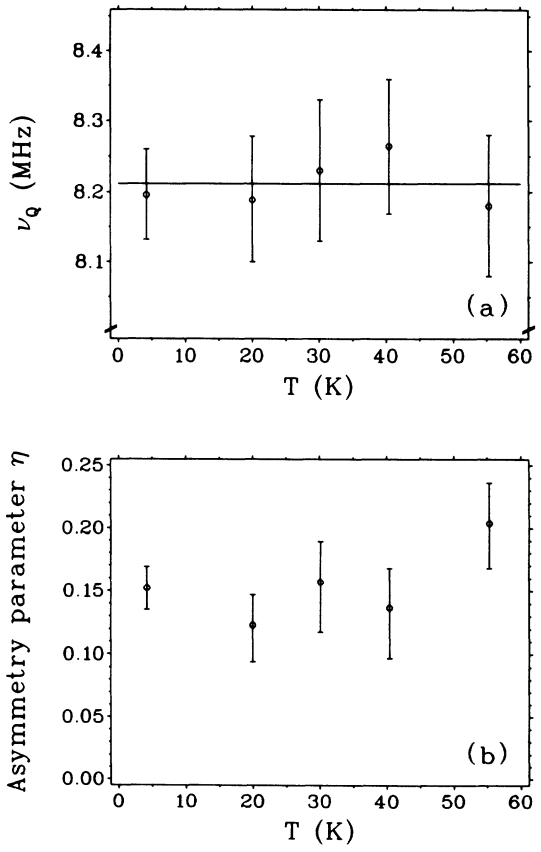

FIG. 4. Change of (a) quadrupole frequency ν_Q and (b) asymmetry parameter η of $^{67}ZnF_2$ with temperature. The change of ν_Q between 4.2 and 55.3 K is smaller than ~1%.

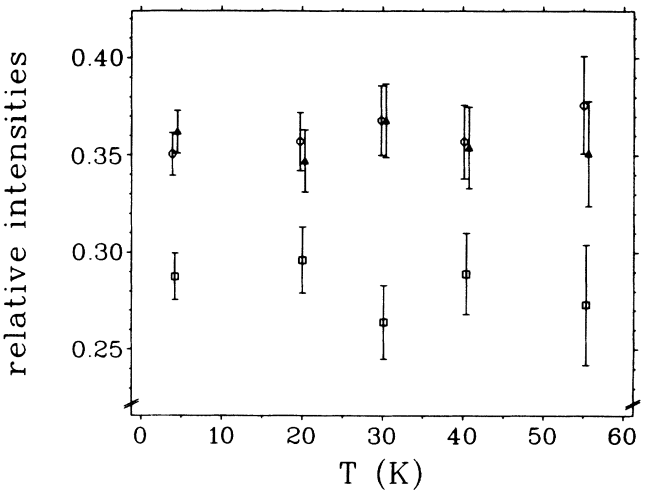

FIG. 5. Relative intensities of the three pairs of absorption lines. □, innermost pair at ~ -40 μm/s; △, pair at ~ -65 μm/s; ○, pair at ~ -100 μm/s (see Fig. 2).

relatively large error in V_{zz} originates mainly from the 10% uncertainty in the quadrupole moment Q.

Contrary to expectation, the EFG tensor in ZnF_2 is at variance with predictions of a simple point charge model,[9] which gives too large a value for η and even the wrong sign for V_{zz}. This discrepancy has been discussed thoroughly in Ref. 8. Recently, detailed theoretical investigations have become available[2,3] which give further insight into these questions. An ionic model is only acceptable if the polarizabilities of the Zn and F ions are allowed for. The experimental results can be reproduced by taking into account even relatively small values for the dipole and quadrupole polarizabilities of the ions. The main component (z axis) of the EFG tensor at the Zn site is predicted to point towards the two nearest F neighbors at the apexes of the distorted octahedron. This model, however, suffers from too many parameters which have to be adjusted to fit the experimental data.

Much more satisfying are cluster calculations also presented in Refs. 2 and 3. The chemical bond is partially covalent due to a rather strong overlap of $3d$, $4d$, $4s$, and $4p$ (Zn) with $2s$ and $2p$ (F) wave functions. The covalent part of the chemical bond causes a charge transfer from F^- to Zn^{2+} which reduces the ionic charges. According to these calculations the EFG at the Zn site (main component $V_{zz}^{\rm calc}\sim +2.4\times10^{17}$ V/cm^2, $\eta^{\rm calc}\sim 0.2$) originates essentially from $4p$, $3d$, and $4d$ electrons. The agreement with our experimental results [$V_{zz}=+(2.25\pm0.23)\times10^{17}$ V/cm^2, $\eta=(0.15\pm0.02)$] is very good. Reference 2 predicts a different orientation of the EFG tensor: surprisingly not the z axis but rather the y axis is pointing towards the F atoms at the apexes, the x axis (z axis) being parallel (perpendicular) to the crystallographic c axis is bisecting the shorter (larger) edges of the basal plane of the octahedron. Unfortunately, from our measurements with ZnF_2 powder we cannot derive the orientation of the EFG tensor. Single crystals made from enriched $^{67}ZnF_2$ would be required. These, however, could be very costly to produce.

B. Center shift

Table I summarizes the results for the temperature dependence of the center shift S_C compared to its value at 4.2 K. A correction was applied to take into account the temperature shift of the ZnO source. Since the temperature of the source stayed always below ~ 18 K, this correction is small. It was calculated using the well-established T^4 dependence for ZnO.[25] In Fig. 6 the negative change of the center shift is plotted versus temperature.

The temperature dependence at constant pressure P of S_C is determined by three contributions[34,35]

$$\left[\frac{\delta S_C}{\delta T}\right]_P=\left[\frac{\delta S_{\rm SOD}}{\delta T}\right]_P+\left[\frac{\delta S}{\delta T}\right]_V+\left[\frac{\delta S}{\delta \ln V}\right]_T\left[\frac{\delta \ln V}{\delta T}\right]_P .$$

The first term describes the second-order Doppler shift (SOD). The second term gives the explicit temperature dependence of the isomer shift S at constant volume V, which may be caused by changes of the s-electron density at the Zn nucleus. The third term represents the volume dependence of S due to thermal expansion of the lattice.

Although there are no high-pressure Mössbauer data on ZnF_2 available at present from which the change of S with reduced volume can be derived, the contribution of the third term to S_C can be estimated to be negligibly small. From thermal expansion coefficients[13,36] for ZnF_2 the total volume change between 4.2 and 55.3 K can be estimated to be smaller than 1×10^{-4}. For ZnO the s-electron density ρ has been calculated[37,38] to vary proportionally to the inverse seventh power of interatomic distance, i.e., $\Delta\rho\approx-\frac{7}{3}(\Delta V/V)\rho$. As an upper limit we take

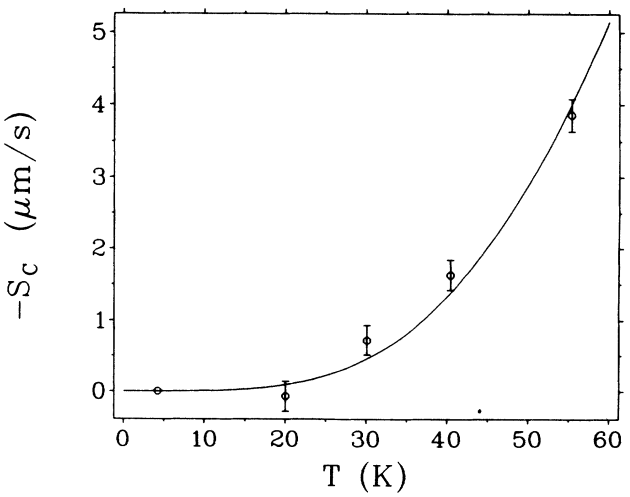

FIG. 6. Temperature dependence of the center shift S_C relative to its value at 4.2 K. The fit by the Debye model (solid line) gives an effective Debye temperature of $\Theta^{S_C}=(278\pm6)$ K.

$\rho = 2.86e/a_H^3$, the full contribution of the 4s electrons.[2] Together with the known value of $\Delta\langle r^2\rangle$ (Ref. 39) we get $\Delta S \sim 0.033$ μm/s, or only $\sim 0.9\%$ of S_C observed between 4.2 and 55.3 K.

The separation of the S_{SOD} from the S_C is a difficult task, the main reason being that the phonon frequency distribution for ZnF_2 is unknown. Specific heat data[40] indicate that optical phonons play a significant role already above ~ 35 K. Still, at lower temperatures the Debye model can be expected to be an acceptable approximation. This indeed appears to be the case: from specific heat data at ~ 12 K an effective Debye temperature $\Theta^{sp} \sim 270$ K is deduced, which then drops to $\Theta^{sp} \sim 240$ K around 35 K. The temperature variation of the Lamb-Mössbauer factor (see below) can well be described by $\Theta^{LMF} = (280 \pm 1)$ K even up to 55.3 K, the highest temperature applied in our investigation. Within the same model the center shift can very well be fitted by $\Theta^{S_C} = (278 \pm 6)$ K. This is demonstrated by the solid line in Fig. 6. Although an explicit temperature dependence of the isomer shift S cannot be excluded completely, the close agreement between the three effective Debye temperatures is a strong hint that the SOD is by far the largest contribution to the temperature variation of S_C. In contrast to ZnO (Ref. 25), the excitation of optical phonons above ~ 35 K prohibits the determination of charge-transfer effects in ZnF_2 at higher temperatures. In the low-temperature limit (4.2 K), however, the change $\Delta\rho(0)$ of the s-electron density at the ^{67}Zn nucleus between $^{67}ZnF_2$ and ^{67}ZnO can be derived. Due to the different Debye temperatures of ZnO ($\Theta = 317.7$ K) (Ref. 25) and ZnF_2 ($\Theta = 280$ K) the second-order Doppler shift gives $S_{SOD} = (8.7 \pm 1.3)$ μm/s. Together with the measured center shift at 4.2 K of $S_C = -(63.44 \pm 0.32)$ μm/s we get for the isomer shift $S = -(72.1 \pm 1.3)$ μm/s. Using the above-mentioned value for $\Delta\langle r^2\rangle$ (Ref. 39) we calculate that $\rho(0)$ in ZnF_2 is reduced with respect to ZnO by $\Delta\rho(0) = 2.1e/a_H^3$. Exactly this value has been predicted in Ref. 2 from cluster calculations which show that $\sim 1.4e/a_H^3$ originate from 4s orbitals whereas the 3s electrons contribute to $\Delta\rho(0)$ by $\sim 0.9e/a_H^3$. The 1s and 2s electrons remain almost unaffected.

C. Anisotropy of the Lamb-Mössbauer factor

As indicated by Fig. 5 the relative intensity (area) I_3 of the innermost pair of absorption lines is $\sim 20\%$ smaller as compared to the outer two pairs, which are about equal. This deviation can be due to anisotropy of the Lamb-Mössbauer factor and/or to texture effects of the absorber. Let us consider texture effects first. Our data show that intensity I_3 originating from the spin $\pm\frac{1}{2} \rightarrow$ spin $\pm\frac{1}{2}$ transitions has to be reduced with respect to the intensities I_1 and I_2 corresponding to the transitions $\pm\frac{1}{2} \rightarrow \pm\frac{5}{2}$ and $\pm\frac{1}{2} \rightarrow \pm\frac{3}{2}$, respectively. This is indeed possible if the crystallites in the absorber exhibit preferred orientation in such a way that the direction of observation of the 93.3-keV γ rays forms an angle of $\sim 90°$ with the direction of the main component of the EFG tensor (axis of quantization). However, in order to fit our experimental results, $\sim 32\%$ of the crystallites would have to be fully oriented in this manner. This appears to be a very large amount for a powder absorber with relatively large geometrical dimensions and crystallites being rather loosely packed. Still, we cannot rule out such texture effects from the beginning.

If we assume that the LMF is isotropic and only texture effects are responsible for the line intensities, the temperature dependence of the LMF f_{iso} and the corresponding mean-square displacements $\langle x_{iso}^2\rangle$ of the ^{67}Zn atom can well be described by a Debye model. This is demonstrated by Table III and Figs. 7 and 8. The solid lines represent a fit giving $\Theta^{LMF} = (280 \pm 1)$ K for the effective Debye temperature. As stated earlier, this value is in surprisingly close agreement with $\Theta^{S_C} = (278 \pm 6)$ K obtained from the temperature dependence of the center shift and with $\Theta^{sp} \sim 270$ K from specific heat data at low temperatures.

The opposite point of view is based on the anisotropy of the LMF. The change of the line intensities is determined only by the Goldanskii-Karyagin effect.[32,33] Texture plays no role. An anisotropic LMF is caused by anisotropic bonding strengths between Zn and its ligands. Not only the rutile structure of ZnF_2, which implies a distorted F octahedron surrounding a Zn atom, but also other physical properties express anisotropic bonding forces. For example, the compressibilities[14,41] parallel (β_c) and perpendicular (β_a) to the c axis as derived from elastic constants[15] differ by a factor of 2 (β_c being smaller) even at 4.2 K. In addition, the values for β_c and β_a are independent of temperature up to 55.3 K within 0.6%.[14] This speaks in favor of a temperature-independent anisotropy of the LMF, which is in agreement with our results.

In order to be more quantitative, we introduce an an-

TABLE III. Temperature dependence of isotropic (f_{iso}) and anisotropic ($f_\parallel$ and $f_\perp$) Lamb-Mössbauer factors as well as the corresponding mean-square atomic displacements of ^{67}Zn in $^{67}ZnF_2$. The anisotropy parameter is given by $B = \mathbf{k}^2(\langle x_\parallel^2\rangle - \langle x_\perp^2\rangle)$.

T_A (K)	f_{iso} (%)	$\langle x_{iso}^2\rangle$ (10^{-3} Å^2)	$f_\parallel$ (%)	$\langle x_\parallel^2\rangle$ (10^{-3} Å^2)	$f_\perp$ (%)	$\langle x_\perp^2\rangle$ (10^{-3} Å^2)	B
4.2	1.23±0.07	1.97±0.02	$0.51^{+0.24}_{-0.16}$	2.36±0.17	$1.74^{+0.25}_{-0.21}$	1.81±0.06	1.23±0.50
20.0	1.09±0.08	2.02±0.03	$0.47^{+0.35}_{-0.20}$	2.40±0.25	$1.54^{+0.32}_{-0.27}$	1.87±0.09	1.20±0.73
30.1	1.02±0.08	2.05±0.04	$0.11^{+0.15}_{-0.07}$	3.06±0.39	$1.99^{+0.39}_{-0.32}$	1.75±0.08	2.9 ±1.0
40.4	0.75±0.06	2.19±0.04	$0.27^{+0.29}_{-0.14}$	2.64±0.32	$1.09^{+0.28}_{-0.22}$	2.02±0.10	1.40±0.93
55.3	0.46±0.04	2.41±0.04	$0.07^{+0.20}_{-0.05}$	3.23±0.58	$0.82^{+0.27}_{-0.21}$	2.15±0.13	2.4 ±1.6

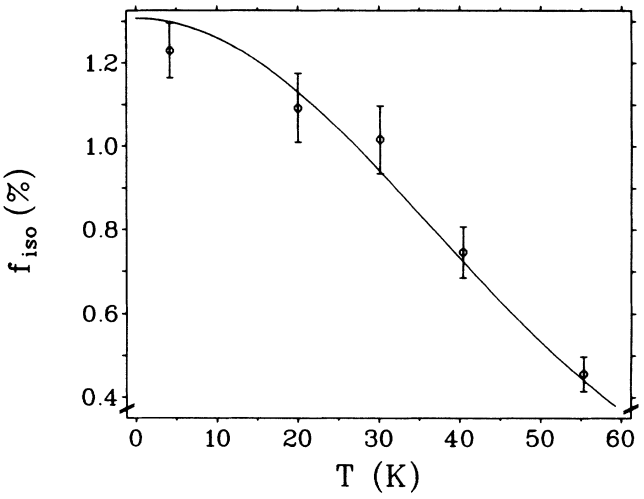

FIG. 7. Temperature dependence of the Lamb-Mössbauer factor. The fit by the isotropic Debye model (solid line) gives an effective Debye temperature of $\Theta^{LMF}=(280\pm1)$ K.

isotropic but axially symmetric LMF (Ref. 21) with $f_{\parallel}$ and $f_{\perp}$ denoting the LMF's parallel and perpendicular to the symmetry axis, respectively. The symmetry axis is taken identical to the main direction of the EFG tensor as discussed above. In such a case the relative intensities of the absorption lines are given by

$$I_1(\pm\tfrac{1}{2}\rightarrow\pm\tfrac{5}{2})\alpha\int_0^1\exp(-Bx^2)\cdot(-10x^4+10)dx ,$$

$$I_2(\pm\tfrac{1}{2}\rightarrow\pm\tfrac{3}{2})\alpha\int_0^1\exp(-Bx^2)\cdot(30x^4-24x^2+10)dx ,$$

$$I_3(\pm\tfrac{1}{2}\rightarrow\pm\tfrac{1}{2})\alpha\int_0^1\exp(-Bx^2)\cdot(-20x^4+24x^2+4)dx ,$$

with the anisotropy parameter $B=\mathbf{k}^2(\langle x_{\parallel}^2\rangle-\langle x_{\perp}^2\rangle)$, where $\mathbf{k}$ is the wave vector of the 93.3-keV γ radiation and $\langle x_{\parallel}^2\rangle$ and $\langle x_{\perp}^2\rangle$ are the mean-square atomic displacements parallel and perpendicular to the main component of the EFG tensor, respectively. The LMF averaged over all orientations of the crystallites in the powder is given by

$$\langle f\rangle=\exp(-C)\int_0^1\exp(-Bx^2)dx ,$$

where $C=\mathbf{k}^2\langle x_{\perp}^2\rangle$.

The LMF $\langle f\rangle$ is determined by the total absorption area of the Mössbauer spectrum and is equal in magnitude to f_{iso}. From the relative intensities of the absorption lines the B value is obtained at each temperature. The results are summarized in Table III. As indicated in Fig. 9, our data give $B\sim1.5$. As compared to Zn metal with $B=3.4$ at 4.2 K and $B=7.9$ at 47 K (Ref. 21) the B value for ZnF_2 is rather low and nearly independent of temperature. Using the results for the B parameter together with the values for $\langle f\rangle$, the mean-square atomic displacements $\langle x_{\perp}^2\rangle$ and $\langle x_{\parallel}^2\rangle$ are derived (see Table III). They are depicted in Fig. 10. The extended Debye model characterized by two Debye temperatures[21] represents the data surprisingly well. The fits (solid lines) give $\Theta_{\parallel}=(229\pm6)$ K and $\Theta_{\perp}=(306\pm4)$ K for the corresponding Debye temperatures. The mean-square atomic displacements as well as the Debye temperatures are significantly different. They reflect the dissimilar bond lengths between the Zn atom and the F ligands at the apexes of the distorted octahedron as compared to the F ligands in the basal plane. The bond lengths differ by $\sim1.7\%$.[11,12]

Also, the change of the center shift S_C with temperature is rather well described by the extended Debye model. However, the temperature dependence of S_C does not provide a critical test of lattice-dynamical models, since, as already mentioned, at higher temperatures charge-transfer effects in ZnF_2 may contribute to S_C via the isomer shift. In summary, without performing experiments

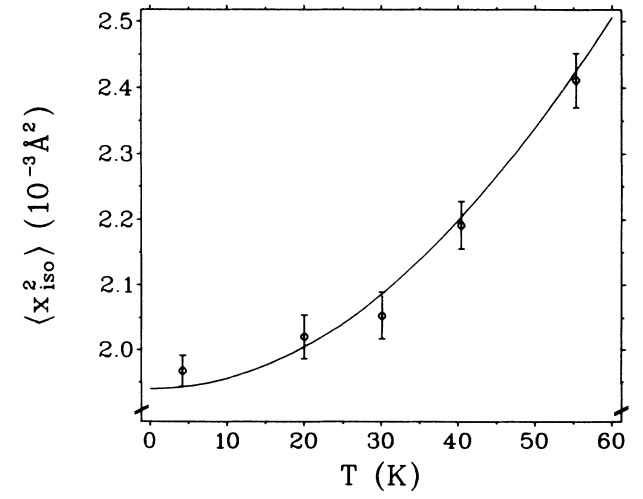

FIG. 8. Isotropic mean-square displacements of ^{67}Zn in $^{67}ZnF_2$ at various temperatures as derived from the Lamb-Mössbauer factor of Fig. 7.

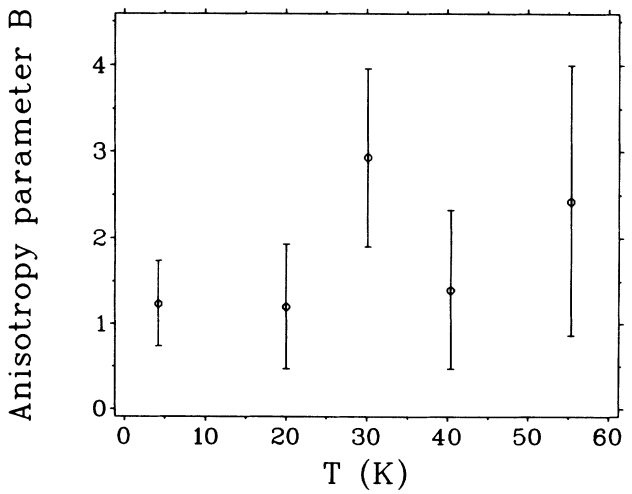

FIG. 9. Temperature dependence of the anisotropy parameter $B=\mathbf{k}^2(\langle x_{\parallel}^2\rangle-\langle x_{\perp}^2\rangle)$.

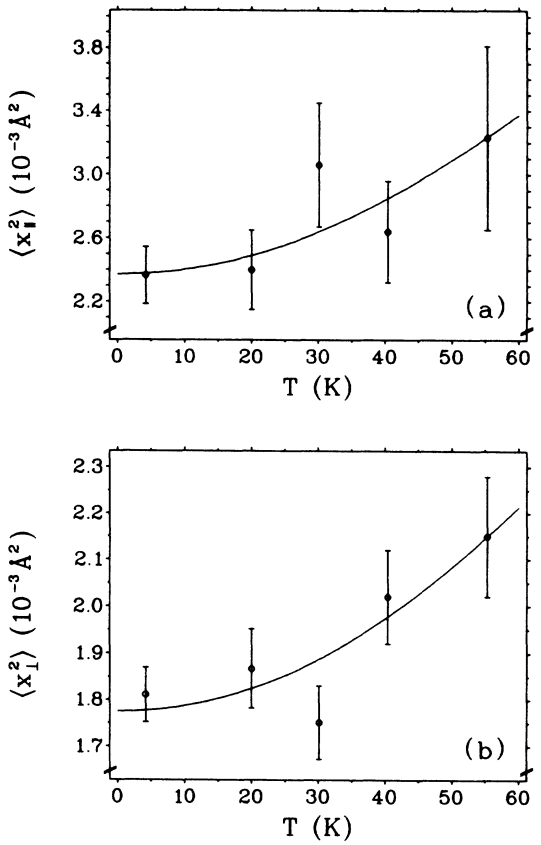

FIG. 10. Temperature dependence of the mean-square displacements of ^{67}Zn in $^{67}ZnF_2$ (a) parallel and (b) perpendicular to the main component of the EFG tensor as described in the text. The solid lines are fits by the extended Debye model with effective Debye temperatures $\Theta_\parallel = 229 \pm 6$ K and $\Theta_\perp = 306 \pm 4$ K.

on ZnF_2 single crystals, we cannot decide if the anisotropic model has to be preferred. Such experiments would also be able to determine the symmetry axes of the LMF and clarify the question if they coincide with the directions of the EFG tensor as was assumed above. From a theoretical point of view the extension of the cluster model[2,3] to calculations of the LMF is most desirable.

Independent of any model for the LMF, our data for ZnF_2 show no indications of a beginning ferroelectric transition. This was proposed[15] to occur at low temperatures accompanied by a soft transverse optical mode (TOM). Since the LMF is very sensitive to the low-frequency part of the phonon distribution such a TOM would easily be seen by a drop of the LMF at low temperatures. Our data exclude this possibility. They support the interpretation of measurements of the dielectric constant[14] where also no hint for a soft TOM could be detected. Therefore the ferroelectric transition most probably does not occur.

V. CONCLUSIONS

The 93.3-keV Mössbauer resonance in $^{67}ZnF_2$ was used to investigate the temperature dependence of the electric quadrupole interaction, the center shift, and lattice-dynamical effects. The electric quadrupole frequency remains independent of temperature within $\sim 1\%$ between 4.2 and 55 K. Both the center shift as well as the Lamb-Mössbauer factor can well be described within the Debye approximation. The question of an anisotropic LMF cannot be answered finally without performing single crystal experiments, although there is considerable evidence for anisotropy. The data on the electric quadrupole interaction as well as on the LMF exclude a proposed ferroelectric transition at low temperatures.

The isomer shift as obtained from the center shift after subtracting the second-order Doppler effect is due to a substantial reduction in s-electron density at the ^{67}Zn nucleus in $^{67}ZnF_2$ as compared to ^{67}ZnO. All hyperfine interactions at 4.2 K are in nice agreement with cluster calculations which have become available recently.

ACKNOWLEDGMENTS

We would like to thank the Kernforschungszentrum Karlsruhe, especially Dr. H. Schweickert, K. Assmus, and W. Maier for numerous and careful source irradiations at the cyclotron. This work has been funded by the German Federal Minister for Research and Technology [Bundesminister für Forschung und Technologie (BMFT)] under Contract No. 03-KA2TUM-4 and by the Kernforschungszentrum Karlsruhe.

[1] A. Svane and E. Antoncik, Phys. Rev. B **33**, 7462 (1986).
[2] S. Nagel, Z. Phys. B (to be published).
[3] H. H. Klauss, N. Sahoo, P. C. Kelires, T. P. Das, W. Potzel, G. M. Kalvius, M. Frank, and W. Kreische, Hyperfine Interact. (to be published).
[4] D. Griesinger, R. V. Pound, and W. Vetterling, Phys. Rev. B **15**, 3291 (1977).
[5] A. Forster, W. Potzel, and G. M. Kalvius, Z. Phys. B **37**, 209 (1980).
[6] A. J. Freeman and D. E. Ellis, in *Mössbauer Isomer Shifts,* edited by G. K. Shenoy and F. E. Wagner (North-Holland, Amsterdam, 1978), p. 111.
[7] W. Potzel, A. Forster, J. Moser, and G. M. Kalvius, Phys. Lett. **88A**, 307 (1982).
[8] W. Potzel and G. M. Kalvius, Phys. Lett. **110A**, 165 (1985).
[9] F. W. de Wette, Phys. Rev. **123**, 103 (1961).
[10] R. W. G. Wyckoff, *Crystal Structures,* 2nd ed. (Wiley, New York, 1965), Vol. 1, p. 250.
[11] W. H. Baur and A. A. Khan, Acta Crystallogr. B **27**, 2133 (1971).
[12] W. H. Baur, Acta Crystallogr. B **32**, 2200 (1976).
[13] K. Haefner, Ph.D. thesis, University of Chicago, 1964 (unpublished).
[14] J. K. Vassiliou, J. Appl. Phys. **59**, 1125 (1986).
[15] D. S. Rimai, Phys. Rev. B **16**, 4069 (1977).
[16] N. Boccara, Ann. Phys. (N.Y.) **47**, 40 (1968).
[17] W. Adlassnig, W. Potzel, J. Moser, W. Schiessl, U. Potzel, C. Schäfer, M. Steiner, H. Karzel, M. Peter, and G. M. Kalvius,

Phys. Rev. B **40**, 7469 (1989).
[18]G. J. Perlow, W. Potzel, R. M. Kash, and H. de Waard, J. Phys. (Paris) **35**, C6-197 (1974).
[19]P. Helistö, E. Ikonen, T. Katila, W. Potzel, and K. Riski, Phys. Rev. B **30**, 2345 (1984).
[20]W. Potzel, Hyperfine Interact. **40**, 172 (1988).
[21]W. Potzel, W. Adlassnig, U. Närger, Th. Obenhuber, K. Riski, and G. M. Kalvius, Phys. Rev. B **30**, 4980 (1984).
[22]Th. Obenhuber, W. Adlassnig, J. Zänkert, U. Närger, W. Potzel, and G. M. Kalvius, Hyperfine Interact. **33**, 69 (1987).
[23]W. Potzel, Th. Obenhuber, A. Forster, and G. M. Kalvius, Hyperfine Interact. **12**, 135 (1982).
[24]G. J. Perlow, L. E. Campbell, L. E. Conroy, and W. Potzel, Phys. Rev. B **7**, 4044 (1973).
[25]C. Schäfer, W. Potzel, W. Adlassnig, P. Pöttig, E. Ikonen, and G. M. Kalvius, Phys. Rev. B **37**, 7247 (1988).
[26]P. Helistö, T. Katila, W. Potzel, and K. Riski, Phys. Lett. **85A**, 177 (1981).
[27]E. Ikonen, P. Helistö, T. Katila, and K. Riski, Phys. Rev. A **32**, 2298 (1985).
[28]W. Potzel and N. Halder, Nucl. Instrum. Methods **226**, 418 (1984).
[29]E. Gerdau, J. Wolf, H. Winkler, and J. Braunsfurth, Proc. R. Soc. London Ser. A **311**, 197 (1969).
[30]N. S. Laulainen and M. N. McDermott, Phys. Rev. **177**, 1606 (1969).
[31]G. K. Shenoy, F. E. Wagner, and G. M. Kalvius, in *Mössbauer Isomer Shifts* (Ref. 6), p. 101.
[32]S. V. Karyagin, Fiz. Tverd. Tela (Leningrad) **8**, 1739 (1966) [Sov. Phys.—Solid State **8**, 1387 (1966)].
[33]S. V. Karyagin, Fiz. Tverd. Tela (Leningrad) **9**, 2514 (1967) [Sov. Phys.—Solid State **9**, 1979 (1968)].
[34]R. V. Pound, G. B. Benedek, and R. Drever, Phys. Rev. Lett. **7**, 405 (1961).
[35]G. M. Rothberg, S. Guimard, and N. Benczer-Koller, Phys. Rev. B **1**, 136 (1970).
[36]G. Diver and A. S. Pavlovic, in *Thermal Expansion 8*, Proceedings of the Eighth International Symposium, Gaithersburg, Maryland, edited by J. V. Sengers (Plenum, New York, 1984), p. 133.
[37]K. N. Shrivastava, Phys. Rev. B **13**, 2782 (1976).
[38]K. N. Shrivastava, Hyperfine Interact. **24-26**, 817 (1985).
[39]F. Buheitel, W. Potzel, and D. C. Aumann, Hyperfine Interact. **47-48**, 606 (1989).
[40]J. W. Stout and E. Catalano, J. Chem. Phys. **23**, 2013 (1955).
[41]J. F. Nye, *Physical Properties of Crystals* (Clarendon, Oxford, 1957), p. 146.